Variable Sphere Molecular Model in the Monte Carlo Simulation of Rarefied Gas Flow

Hiroaki Matsumoto

Division of Systems Research, Yokohama National University
79-5 Tokiwadai, Hodogaya, Yokohama 240-8501, Japan

Abstract. The variable sphere (VS) molecular model is introduced to Monte Carlo simulation of rarefied gas flow. The VS model provides the consistency for diffusion and viscosity cross-sections with those of any realistic intermolecular potential. The VS model has a much simpler scattering law than either the variable hard sphere (VHS) or variable soft sphere (VSS) models; also, it has the same computational efficiency as the VHS and VSS models. In this study, VS model is applied to the inverse power law (IPL) and Lennard-Jones (LJ) potentials. Comparative simulations between the VS mode, IPL and LJ potentials are made for the molecular diffusion in a homogeneous heat-bath gas, normal shock wave structure in a monatomic gas, and normal shock wave structure in binary gas mixture. The good agreement is shown in the molecular diffusion and shock wave structure between the VS model and the IPL and LJ potentials. The VS model is applied to the statistical inelastic cross-section (SICS) model for the rotational inelastic collision of the diatomic molecule. Comparative simulation between the VS model with the SICS (VS-SICS) model and VSS model with SICS (VSS-SICS) model is made for rotational relaxation in a nitrogen normal shock wave. The agreement in the shock wave structure and rotational energy distribution function across the shock wave between the VS-SICS model and the VSS-SICS model are good. It is shown that the macroscopic transport phenomena are affected by the diffusion and viscosity cross-sections rather than the scattering law of the each molecular collision.

INTRODUCTION

The Monte Carlo method[1,2] has been developed[3,4] and widely applied to a variety of rarefied gas flow problems because of its accuracy, efficiency, and simplicity. For engineering, realistic and effective molecular collision models are required. The variable hard sphere (VHS) molecular model[5,6] is attractive as a simple and efficient realistic collision model and applied to a lot of rarefied gas flow problems. The VHS model is suggested for the inverse power law (IPL) potential for the first time, and then extended to a more realistic intermolecular potential such as Lennard-Jones (LJ) potential[7,8]. Previous papers[9,10], pointed out, however, that either the diffusion cross-section (diffusion coefficient) or the viscosity cross section (viscosity coefficient) of the VHS model is inconsistent with that of the potential, such as IPL and LJ potentials. In order to overcome this problem, the variable soft sphere (VSS) molecular model[11,12], is introduced for both the diffusion cross-section (diffusion coefficient) and viscosity cross-section (viscosity coefficient) to be consistent with any realistic intermolecular potential and applied to the IPL and LJ potentials. From the basic concepts of the VHS and VSS models, many simple and realistic molecular collision models should be constructed. In this study, the variable sphere (VS) molecular model is introduced for both diffusion and viscosity cross-sections to be consistent with any realistic intermolecular potential and applied to IPL and JL potentials. The scattering law of the VS model is simpler than that of the VHS and VSS models and computational efficiency is almost identical to VHS and VSS models. Comparative calculations between the VS model and IPL and LJ potentials are made for the molecular diffusion in a homogeneous heat-bath gas and normal shock-wave structure in a monatomic gas and normal shock wave structure in binary gas mixture. For the VS model for IPL potential, the Maxwell molecule and hard sphere are chosen as practical models for softness and hardness. The VS model for IPL potential is applied to the statistical inelastic cross-section (SICS) model[13,14] and comparative calculation between the VS model with the SICS model (VS-SICS) and VSS model with SICS model (VSS-SICS) is made for rotational relaxation in a nitrogen normal shock wave structure.

CP663, *Rarefied Gas Dynamics: 23rd International Symposium*, edited by A. D. Ketsdever and E. P. Muntz

VARIABLE SPHERE MOLECULAR MODEL

Scattering Law and Cross-Sections

The VS molecular model has definite diameter d, which varies with molecular relative collision energy ε and scatters with the same deflection angle $\chi = \chi_0$ for effective impact parameter b, defined as

$$\chi = \begin{cases} \chi_0 & (b \le d) \\ 0 & (b > d) \end{cases}. \tag{1}$$

The total cross-section of the VS model is obtained as

$$\sigma_t = 2\pi \int b db = \pi d^2 . \tag{2}$$

Diameter d (or total cross-section σ_t) and deflection angle χ_0 are defined so that both diffusion and viscosity cross-sections are consistent with those of a realistic intermolecular potential. The VS model diffusion and viscosity cross-sections are defined as

$$Q^{(1)} = 2\pi \int (1-\cos\chi) b db = (1-\cos\chi_0)\pi d^2 \quad \text{and} \tag{3}$$

$$Q^{(2)} = 2\pi \int (1-\cos^2\chi) b db = (1-\cos^2\chi_0)\pi d^2 , \tag{4}$$

respectively. From equations (3) and (4), total cross-section and cosine of deflection angle χ_0 are uniquely obtained as

$$\sigma_t = \pi d^2 = \frac{Q^{(1)}}{2Q^{(1)} - Q^{(2)}} Q^{(1)} \quad \text{and} \tag{5}$$

$$\cos\chi_0 = \frac{Q^{(2)} - Q^{(1)}}{Q^{(1)}} , \tag{6}$$

respectively. Equations (5) and (6) show that total cross-section and deflection angle of the VS model are defined from diffusion and viscosity cross-sections of any realistic intermolecular potential.

VS Model for IPL Potential

Diffusion and viscosity cross-sections for IPL potential with intermolecular force $F=\kappa r^{-v}$ are given as

$$Q^{(1)} = 2\pi A_1(v) \left(\kappa/2\right)^{2/(v-1)} \varepsilon^{-2/(v-1)} \quad \text{and} \tag{7}$$

$$Q^{(2)} = 2\pi A_2(v) \left(\kappa/2\right)^{2/(v-1)} \varepsilon^{-2/(v-1)} , \tag{8}$$

respectively, where κ is the force constant, v is the exponent of the intermolecular distance r, and $A_1(v)$ and $A_2(v)$ are integrals defined in Ref. 15; numerical values are given in Refs. 11 and 15.

Substituting Eqs. (7) and (8) into Eqs. (5) and (6), the total cross-section and deflection angle cosine of the VS model for IPL potential are obtained as

$$\sigma_t = \frac{2\pi A_1(v)^2}{2A_1(v) - A_2(v)} \left(\frac{\kappa}{2}\right)^{\omega} \varepsilon^{-\omega}, \tag{9}$$

$$\cos\chi_0 = \frac{A_2(v) - A_1(v)}{A_1(v)}, \text{ and} \tag{10}$$

$$\omega = 2/(v-1) . \tag{11}$$

Figure 1 (a) shows the VS model deflection angle χ_0 / π as a function of relative collision energy exponent ω. The deflection angle decreases monotonously with increasing relative collision energy exponent ω.

VS model for LJ potential

Diffusion and viscosity cross-sections for Lennard-Jones(6-12) potential,

$$\phi(r) = 4\varepsilon_{LJ}\left[\left(d_{LJ}/r\right)^{12} - \left(d_{LJ}/r\right)^{6}\right], \tag{12}$$

are given numerically, where ε_{LJ} is depth of the potential well and d_{LJ} is the value of intermolecular distance at $\Phi = 0$. Numerical values of reduced diffusion cross-section $Q^{(1)*}=Q^{(1)}/(\pi d_{LJ}^2)$ and viscosity cross-section $Q^{(2)*}=Q^{(2)}/(2\pi d_{LJ}^2/3)$ over the reduced relative collision energy $\varepsilon/\varepsilon_{LJ}$ are calculated using a quadrature scheme[11]. The total cross-section and cosine of deflection angle of the VS model for the LJ potential are obtained as

$$\sigma_t = \frac{3Q^{(1)*2}}{6Q^{(1)*} - 2Q^{(2)*}} \text{ and} \tag{13}$$

$$\cos\chi_0 = \frac{2Q^{(2)*} - 3Q^{(1)*}}{3Q^{(1)*}}. \tag{14}$$

Figure 1(b) shows the variation of deflection angle χ_0/π as a function of reduced relative collision energy $\varepsilon/\varepsilon_{LJ}$

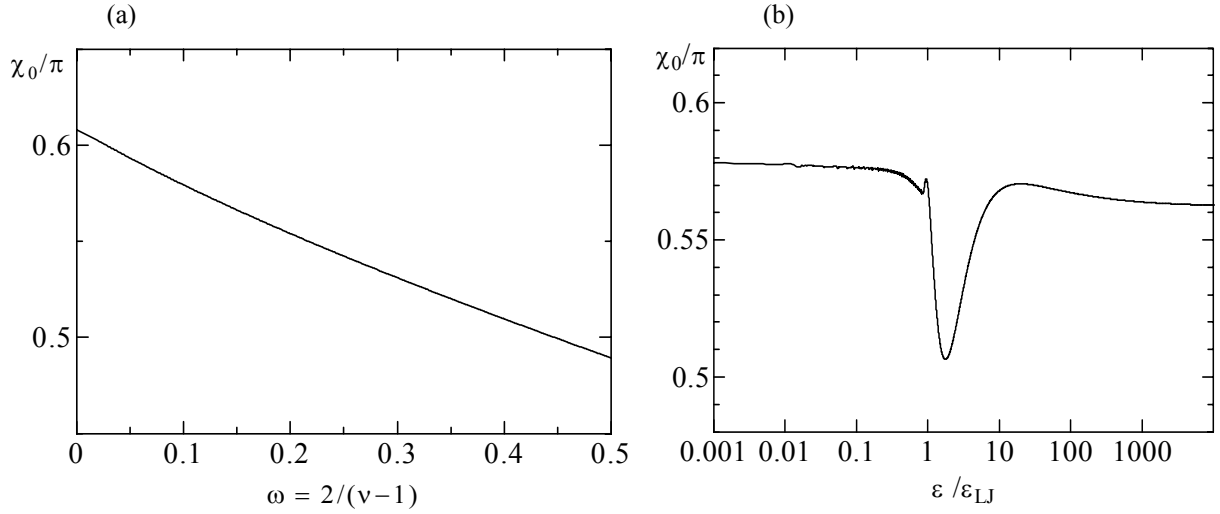

FIGURE 1. Deflection angle of the VS model. (a) VS model for IPL potential as a function of relative collision energy exponent ω. (b) VS model for Lennard-Jones potential as a function of reduced relative collision energy $\varepsilon/\varepsilon_{LJ}$.

COMPARISON BETWEEN VS MODEL AND IPL AND LJ POTENTIALS

Molecular Diffusion in a Homogeneous Heat-Bath Gas

Comparative calculations between the VS model and the IPL and LJ potentials are made for molecular diffusion of trace molecules in a homogeneous heat-bath gas of molecular mass M, number density n, and equilibrium temperature T. Trace molecules of molecular mass m are assumed not to interact mutually and to collide with molecules in heat-bath gas, which keeps the equilibrium Maxwellian velocity distribution. Initially, positions of all trace molecules are taken as the origin of position vector $\boldsymbol{r} = \mathbf{0}$; velocities are assigned by equilibrium Maxwellian distribution at temperature T_0, respectively. Time evolution of position and velocity of each trace molecule are simulated by the test particle Monte Carlo technique[4]. The diffusion coefficient of the trace molecule is calculated from the steady state time gradient of the radial mean square of displacement of each molecule, defined by[16]

$$D = \frac{1}{6}\frac{d\left\langle r^2\right\rangle}{dt}. \tag{15}$$

In this study, the deflection angle for the IPL and LJ potentials is calculated by the procedure in Ref. 17; the cutoff deflection angle $|\chi_{\min}|$ is taken as 1°. The number of trace molecules is taken as $N=10^5$ and the temperature ratio and mass ratio are taken as $T_0/T=1$, and $M/m=1$, respectively. Figure 2(a) shows comparison of evolution of radial mean-square displacement $<(r/\lambda_{IPL})^2>$ of trace molecules versus time $t\cdot c_m/\lambda_{IPL}$ between the VS model and IPL potential for Maxwell molecule and hard sphere, where $c_m=(2k_BT/M)^{1/2}$ is the most probable thermal velocity in the homogeneous heat-bath gas and λ_{IPL} is the mean free path for IPL potential in the homogeneous heat-bath gas, defined as

$$\lambda_{IPL}=\left(16\eta/5n\right)\left(2\pi Mk_BT\right)^{-1/2}, \tag{16}$$

where k_B is Boltzmann constant and η is viscosity of heat-bath gas.

Agreement with diffusion for the VS model and IPL potentials for Maxwell molecule and hard sphere is quite good. The steady state time gradient of $<(r/\lambda_{IPL})^2>$ is established at $t\cdot c_m/\lambda_{IPL}\geq 10$. Evolution of $<(r/\lambda_{LJ})^2>$ versus $t\cdot c_m/\lambda_{LJ}$ is compared in Fig. 2(b) for heat-bath gas temperatures T=10 K, 300 K, and 1000 K between the VS model and LJ potential with ε_{LJ}/k_B=124 K and d_{LJ}=3.418 *Å* for argon gas[18], where λ_{LJ} is the mean free path in the homogeneous heat-bath gas for LJ potential, defined as

$$\lambda_{LJ}=\left(\sqrt{2}\pi d_{LJ}^2 n\right)^{-1}, \tag{17}$$

Differences between molecular diffusion for the VS model and the LJ potential are indistinguishable and the steady state time gradient of $<(r/\lambda_{LJ})^2>$ is established at $t\cdot c_m/\lambda_{LJ}\geq 10$. Normalized diffusion coefficients $6D/(c_m\cdot\lambda_{IPL})$ of the VS model, IPL potential and Chapman-Enskog (CE) solution of the second order approximation for the Maxwell molecule and hard sphere are summarized in Table 1; $6D/(c_m\cdot\lambda_{LJ})$ of the VS model, LJ potential and CE solution of the second order approximation are summarized in Table 2.

The diffusion coefficient of the VS model, IPL and LJ potential agree remarkably well with the CE solution.

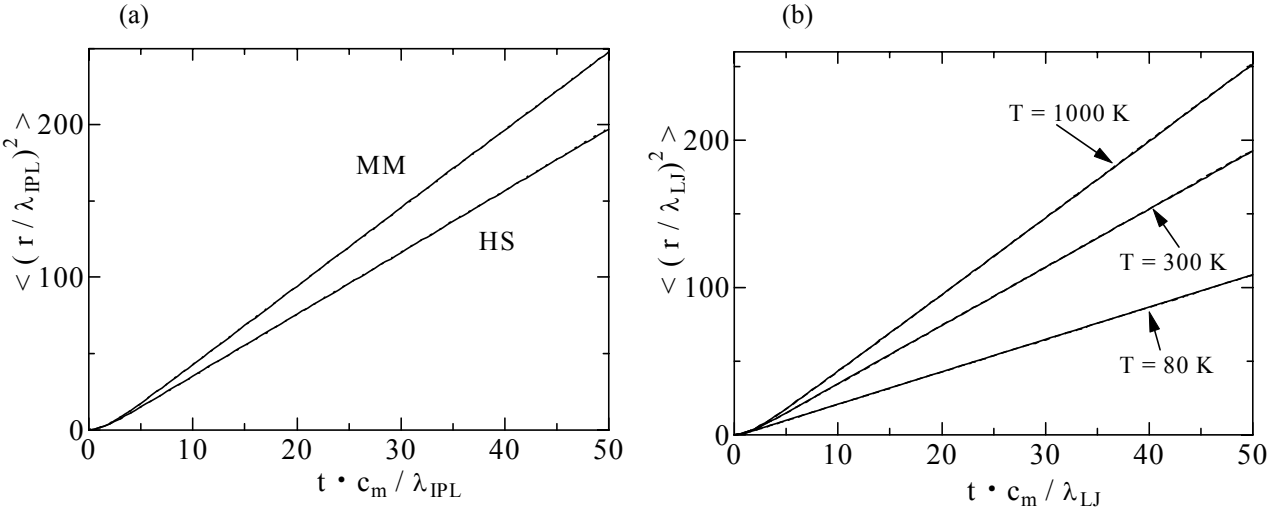

FIGURE 2. Time evolution of radial mean-square displacement of trace molecules in a heat bath gas. (a) IPL potential for hard sphere and Maxwell molecule, (b) Lennard-Jones potential for heat-bath temperature 80, 300, 1000 K.

TABLE 1. Comparison of normalized diffusion coefficient between the VS model, IPL potential for hard sphere (HS;ω=0) and Maxwell molecules (MM;ω=0) and Chapman-Enskog solution of the second order approximation (CE).

ω	IPL	VS	CE
0.0 (HS)	4.076	4.053	4.057
0.5(MM)	5.130	5.130	5.145

TABLE 2. Comparison of normalized diffusion coefficient between the VS model, LJ potential and Chapman-Enskog solution of the second order approximation (CE) for temperature of the homogeneous heat-bath gas T=80 K, 300 K, and 1000 K.

T [K]	LJ	VS	CE
80.0	2.199	2.211	2.209
300.0	3.970	3.953	3.953
1000.0	5.229	5.215	5.218

Normal Shock Wave Structure in a Monatomic Gas

Comparative calculations between the VS model and the IPL and LJ potential are made for the normal shock wave structure in a simple gas. The flow field is regarded as one-dimensional and coordinate x is taken to be flow direction. The computational domain is taken as $-x_0/\lambda_1 \le x/\lambda_1 \le x_0/\lambda_1$, and divided into the collision and data cell $\Delta x/\lambda_1$. Here, λ_1 is the upstream mean free path, defined as

$$\lambda_1 = \left(16\eta_1 / 5n_1\right)\left(2\pi m k_B T_1\right)^{-1/2}, \tag{18}$$

where subscript 1 represents the upstream equilibrium state. Initially, a discontinuous surface is taken at the origin of coordinate x; i.e. a large number of molecules are uniformly distributed with upstream equilibrium Maxwellian velocity distribution for $x/\lambda_1 \le 0$, and with down stream equilibrium Maxwellian velocity distribution for $x/\lambda_1 \ge 0$. Upstream and downstream equilibrium states are connected with the Rankine-Hugoniot relation. Influx molecules across upstream and down stream boundaries are assigned by boundary conditions of upstream and down stream equilibrium Maxwellian distribution, respectively. Time evolution of positions and velocities of each molecule are simulated basically by the same algorithm in Ref. 1, except for treatment of estimating molecular collisions. In this study, collision sampling is conducted using the null-collision technique[3,4]. After the steady state shock wave is established, flow properties are calculated and averaged until statistical fluctuations become sufficiently small. Figures 3(a) and 3(b) show a comparison of normalized number density $(n-n_1)/(n_2-n_1)$ and normalized temperature $(T-T_1)/(T_2-T_1)$ profiles for upstream Mach number M_1=10 between the VS model and IPL potential for Maxwell molecule and hard sphere, respectively, where the subscript 2 denotes the down stream equilibrium state. Calculation domain and collision cell size are taken as x_0/λ_1=100 and $\Delta x/\lambda_1$=1 for Maxwell molecule and x_0/λ_1=20 and $\Delta x/\lambda_1$=0.05 for hard sphere, respectively. Shock wave profiles of the VS model agree well with those of the IPL potential, though there is a slight difference in initial increase of the temperature profile between the VS model and the Maxwell molecule. It is notable that velocity distribution function of the VS model is different from that of IPL potential and that macroscopic profiles are influenced by the diffusion and viscosity cross-sections rather than scattering law.

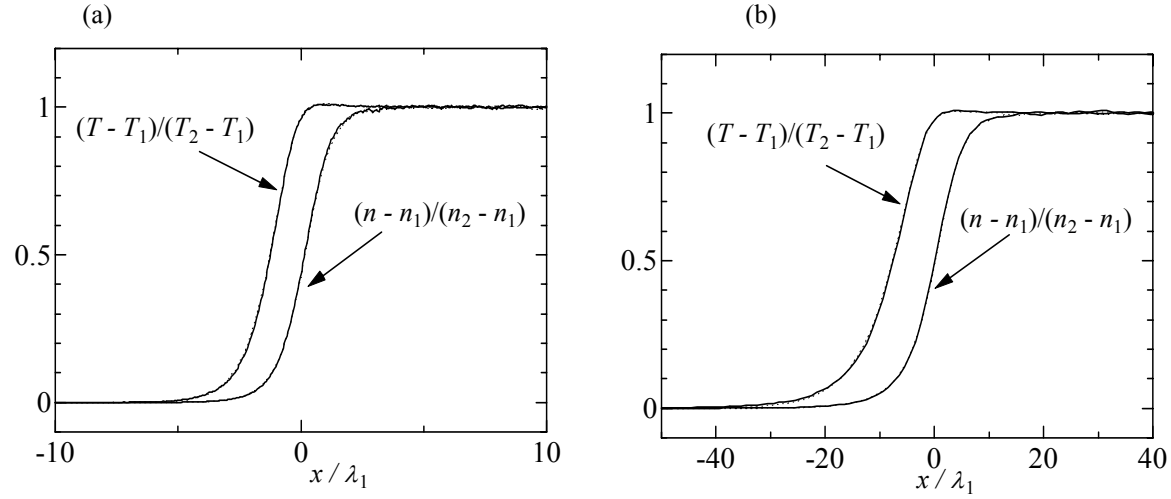

FIGURE 3. Comparison of shock wave profiles between the VS model (solid line) and IPL potential (broken line) for upstream Mach number M_1 =10. (a) hard sphere, (b) Maxwell molecule.

Number density and temperature profiles for upstream Mach number M_1=7.183 and upstream temperature T_1=16 K are compared in Fg. 4 (a) between the VS model and LJ potential with ε_{LJ}/k_B=124 K and d_{LJ}=3.418 Å for argon gas. Calculation domain and collision cell size are taken as x_0/λ_1=50 and $\Delta x/\lambda_1$=0.1, respectively. Difference of shock wave profiles between the VS model and LJ potential is negligible; also, macroscopic profiles are influenced by the diffusion and viscosity cross-sections rather than the scattering law, consistent with the case of IPL potential. However, the velocity distribution function of the VS model is different from that of the LJ potential,which is same as in the case of the IPL potential. Figure 4 (b) shows comparison of parallel velocity distribution function (VDF) in a shock wave at normalized number density $(n-n_1)/(n_2-n_1)$=0.5. The VDF of the VS model forms bimodal distribution which is represented approximately by the merging of two Maxwellian distribution functions at the upstream and down stream equilibrium state.

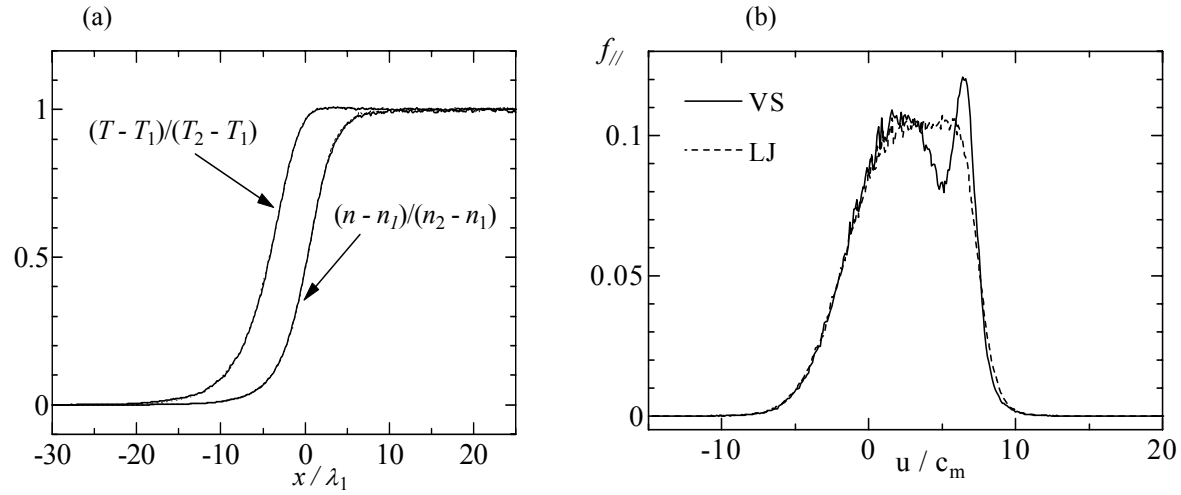

FIGURE 4. Comparison of shock wave profiles between the VS model (solid line) and LJ potential (broken line) for upstream Mach number M_1=7.183. (a) number density and temperature, (b) parallel velocity distribution function at $(n-n_1)/(n_2-n_1)$=0.5.

Normal shock wave structure in binary gas mixture

Comparative calculations between the VS model and LJ potential are made for the normal shock wave structure in helium (He) - xenon (Xe) binary gas mixture. The flow field is regarded as one-dimensional and coordinate x is taken to be flow direction. The computational domain is taken as $-25 \le x/\lambda_{He1} \le 25$ and divided into the collision and data cell $\Delta x/\lambda_{He1}$=0.2. Here, λ_{He1} is the upstream mean free path of helium gas, defined as,

$$\lambda_1 = \left(16\eta_{He1} / 5n_{He1}\right)\left(2\pi m_{He} k_B T_1\right)^{-1/2}, \tag{19}$$

where η_{He1} and n_{He1} are the upstream viscosity and number density of He, respectively and m_{He} is the molecular mass of He. Formation of a steady-state normal shock wave is identical to simulation of a monatomic gas. Figures 5 (a) and 5 (b) show comparison of normalized number density and temperature profiles of He and Xe between the VS model and LJ potential for upstream Mach number M_1=3.89, temperature T_1=300 K, and mole fraction of xenon f_{Xe}=0.03 with d_{LJ}=2.576 Å, ε_{LJ}/k_B= 10.22 K, m_{He}=4.0026 mu, for helium gas and d_{LJ}=4.055 Å, ε_{LJ}/k_B= 229.0 K, m_{Xe}=131.29 mu for xenon gas. The potential parameters between helium and xenon are estimated by the combining laws. The agreement of the shock wave profiles between the VS model and LJ potential are remarkably good.

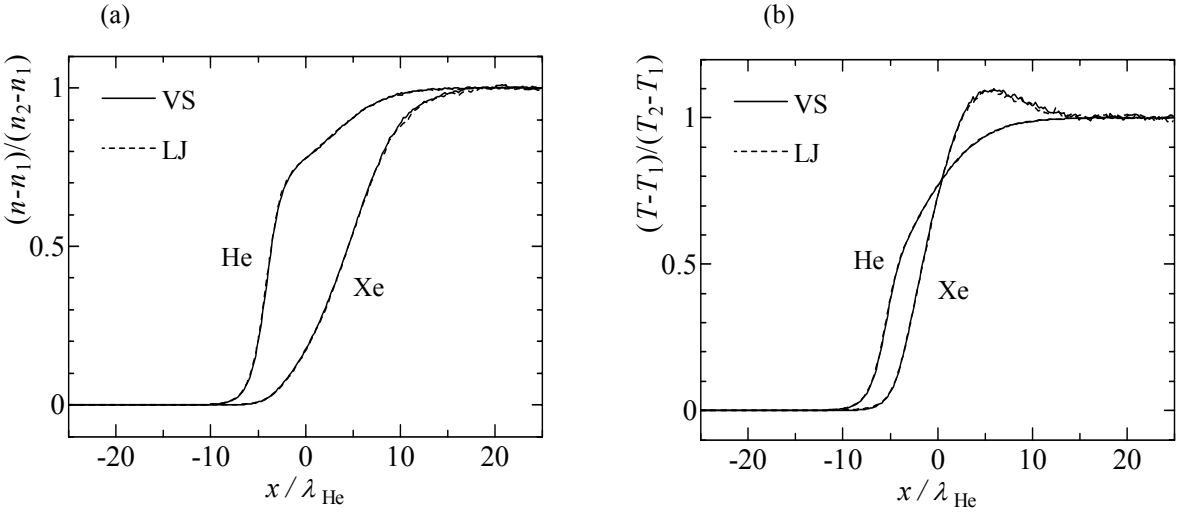

FIGURE 5. Comparison of shock profiles between the VS model and LJ potential for upstream Mach number M_1 =3..89, temperature T_1=300 K and mole fraction of xenon f_{xe}=0.03. (a) normalized density (b) normalized temperature

APPLICATION TO THE INELASTIC MOLECULAR COLLISION MODEL

The VS model for IPL potential is combined with the statistical inelastic cross-section (SICS) model for continuous rotational energy. The total cross-section σ_t for the SICS model is defined as

$$\sigma_t = \sigma_{el} + \sigma_R \text{ and} \tag{20}$$

$$\sigma_R\left(\varepsilon, \xi_1, \xi_2\right) = Z\left(E\right)\sigma_{el} \ , \tag{21}$$

where σ_{el} and σ_R are elastic and inelastic rotational cross-sections; ξ_1, ξ_2 and $E=\varepsilon+\xi_1+\xi_2$ represent rotational energy of collision molecules and total energy for rotationally inelastic collision, respectively. Function $Z(E)$ is defined as

$$Z\left(E\right)\begin{cases}(4-\omega)\Delta E\left(E\right)/E & E \geq E_{th} \\ 0 & E < E_{th}\end{cases} \text{ and} \tag{22}$$

$$\Delta E = \left[E/2 + (2\pi/3)\left(EE^*\right)^{1/2} + \left(2+\pi^2/4\right)E^*\right]/Z_r^{\infty} \ , \tag{23}$$

where E_{th} is threshold energy and $\Delta E(E)$ is Parker's rotational energy gain function par flux molecules[19]; E^* and Z_r^{∞} are constant parameters. Comparative calculation between the VS model with the SICS model (VS-SICS) and the VSS model with the SICS model (VSS-SICS) are made for the nitrogen normal shock wave structure with parameters[20] of E_{th}/k_B =17.18 K, E^*/k_B= 79.8 K, Z_r^{∞}=21, and ω=0.359. It should be noted that the inelastic rotational cross-section of VS-SICS model should be modified so that the inelastic rotational collision frequency (or cross-section) is equal to the VSS-SICS model; i.e. $[\sigma_R]_{VS} = [\sigma_R]_{VSS}$. The flow field is regarded as one-dimensional and coordinate x is taken to be flow direction. The computational domain is taken as $-30 \leq x/\lambda_1 \leq 30$ and divided into the collision and data cell $\Delta x/\lambda_1$=0.1. Here, λ_1 is the upstream mean free path, defined as

$$\lambda_1 = \left(16\eta_1/5n_1\right)\left(2\pi m k_B T_1\right)^{-1/2}, \tag{24}$$

where η is the viscosity coefficient for the molecular collision without internal energy, and subscript 1 represents the upstream equilibrium state. Formation of a steady-state normal shock wave is identical to simulation of a monatomic gas. Normalized number density $(n-n_1)/(n_2-n_1)$, normalized translational temperature $(T_{tr}-T_1)/(T_2-T_1)$, and normalized rotational temperature $(T_R-T_1)/(T_2-T_1)$ profiles of the VS-SICS and VSS-SICS models are compared in Fig. 6 (a) for the upstream Mach number M_1=7.0 and temperature T_1=23.0 K. Normalized number density and rotational temperature profiles of the VS-SICS model agree well with those of the VSS-SICS; however, slight discrepancies are observed in translational temperature profiles. Figures 6 (b) shows comparison of rotational energy distribution between the VS-SICS model and VSS-SICS model through a Mach number M_1=7.0 shock wave. Agreement of rotational energy distributions for VS-SICS and VSS-SICS are very good. It should be noted that macroscopic profiles and rotational energy distribution in a shock wave structure of diatomic molecules are also influenced by the diffusion and viscosity cross sections rather than the scattering law, consistent with the case of the simple gas; rotational collision frequency, moreover rotational cross-section affects macroscopic structure and rotational energy distribution in a shock wave in diatomic molecules.

CONCLUDING AND REMARKS

The variable sphere molecular model is introduced to Monte Carlo simulation of rarefied gas flow. Diffusion and viscosity cross-sections of the VS model are consistent with those of any intermolecular potential; furthermore, computational efficiency is almost identical to VHS and VSS models. In this paper, the VS model is introduced to the IPL and LJ potentials and applied to simulation of molecular diffusion in a homogeneous heat-bath gas and normal shock wave structure in a simple gas; it is then compared with calculation results of IPL and LJ potentials. Good agreement is shown for molecular diffusion and shock wave structure between the VS model and IPL; also, the LJ potentials are very good. To examine applicability to simulation of rotational relaxation of diatomic molecules, the VS model is combined with the SICS model and applied to simulation of rotational relaxation in the nitrogen normal shock wave structure and compared with calculation results of the VSS with SICS model. Shock profiles of number density, rotational temperature, and rotational energy distribution in the shock wave for the VS model agree well with those for VSS model, although there is a slight difference in translational temperature profiles. The VS model demonstrated applicability to the inelastic molecular collision model.

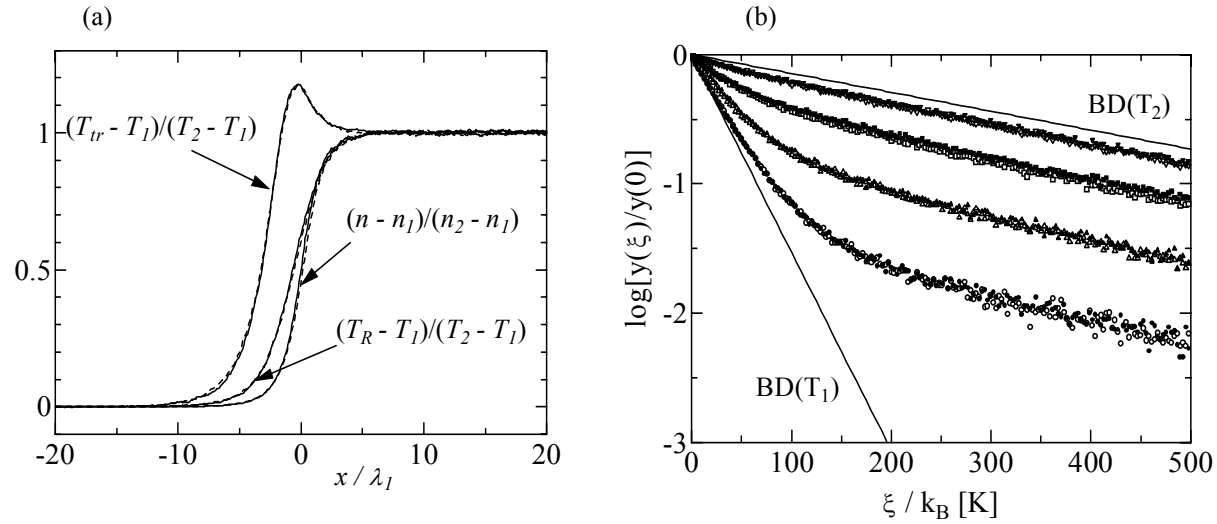

FIGURE 6. Comparison of shock wave profiles between VS-SICS model (solid line and solid symbol) and VSS-SICS model (broken line and open symbol) for upstream Mach number M_1=7 nitrogen shock wave. (a) normalized number density, translational temperature, and rotational temperature. (b) Relaxation of relative rotational energy distribution in a shock wave at x / λ_1=-2.05 (●,○) , x / λ_1=-0.35 (▲,Δ) , x / λ_1=0.95 (■,□) , x / λ_1=2.05 (▼,∇).

REFERENCES

1. Bird, G.A., *Molecular Gas Dynamics*, Clarendon, Oxford, 1976.
2. Bird, G.A., *Molecular Gas Dynamics and the Direct Simulation of Gas Flow*, Clarendon, Oxford, 1994.
3. Koura, K., Phys. of Fluids **29,**3509-3511 (1986).
4. Koura, K., "Null Collision Monte Carlo Method:Gas Mixtures with Internal Degrees of Freedom and Chemical Reactions," in *Prog. Astronaut. Aeronaut*. Edited by E. P. .Muntz, AIAA 117, Washington, DC, 1989 pp.25-39.
5. Bird, G.A., "Monte Carlo Simulation in an Engineering Context," in *Prog. Astronaut. Aeronaut.* Edited by S. S. Fisher, AIAA 74, New York, New York, 1981, pp.239-255 .
6. Bird, G.A., *Phys. Fluids* **26,** 3222-3223 (1983).
7. Hassan, H.A. and Hash, D.B., *Phys. Fluids* **A5,** 738-744 (1993).
8. Matsumoto, H. and Kobayashi, T., *Trans. Jpn. Soc. Mec. Eng.* **60,** 1269-1274 (1994).
9. Koura, K., Matsumoto, H. and Shimada, T., *Phys. Fluids* **A3,** 1835-1837 (1991).
10. Matsumoto, H. and Koura, K., "Monte Carlo Simulation of Normal Shock Wave in Binary Gas Mixtures Using the Variable Soft-Sphere Molecular Model," in *Prog. Astronaut. Aeronaut.* edited by B. D. Shizgal et al., AIAA 158, Washington, DC, 1994, pp.413-423.
11. Koura, K. and Matsumoto, H., *Phys. Fluids* **A3,** 2459-2465 (1991).
12. Koura, K. and Matsumoto, H., *Phys. Fluids* **A4,** 1083-1085 (1992).
13. Koura, K., *Phys. Fluids* **A4,** 1782-1788 (1992).
14. Koura, K., *Phys. Fluids* **A5,** 778-780 (1993).
15. Chapman, S. and Cowling, T.G., *The Mathematical Theory of Non-Uniform Gases,* Cambridge Univ. Press, 1976
16. MacQarrie, D.A., *Statistical Mechanics*, University Science Book, California, 2000.
17. Baker, J.A., Fock,W. and Smith, F., *Phys. Fluids* **7,** 897-903 (1964).
18. Hirschfelder, J.O., Curtiss, C.F. and Bird, R.B., *Molecular Theory of Gases and Liquids,* Wiley, New York 1963.
19. Parker, J.G., *Phys. Fluids* **2,** 449-462 (1959).
20. Koura, K., *Computers Math. Applic*. **35,** 139-154 (1998).